Performance Evaluation of Off Grid Hybrid Distribution System with ANFIS Controller

Naga Venkata Karthik Gandham and Pragaspathy Subramani(✉)

Electrical and Electronics Engineering, Vishnu Institute of Technology, Bhimavaram, Andhra Pradesh 534202, India
pathyeee@yahoo.co.in

Abstract. Off-grid hybrid distribution systems are innovative and environmentally friendly ways to address the energy needs of remote or isolated communities or facilities by combining a number of power generation and energy storage sources. These systems are made to function independently from the primary electrical grid, which makes them perfect for areas with little or no access to centralized electrical infrastructure. In this work, designed an effective microgrid system with integration of distributed power sources such as wind turbine and Photovoltaic system (PV). Moreover, adaptive neuro fuzzy inference system (ANFIS) is developed in this study to track the maximum power from PV panels under various uncertain conditions. Further, due to intermittent nature of the wind speed and irradiance levels, battery system is designed in this work for stable and reliable operation of microgrid system. Moreover, the battery performance and ANFIS-based maximum power point tracking (MPPT) are investigated. As per simulation findings, ANFIS based MPPT approach provides an effective outcome in terms of settling time, efficiency and accuracy in suggested microgrid systems.

Keywords: Microgrid · ANFIS · PMSG · MPPT · Battery Bank

1 Introduction

Smart city is the state of art for the modern day living and perhaps it influences the unbounded technology to roll over the culture and certainly enhances the functional outcomes via vital information and communication. Internet of Things (IoT) on the other hand, sustains the aforementioned concept of smart city and invites wider adoption in the sectors like transportation, shadowing, disaster monitoring, natural calamities, electrifications, public and private analytics etc. Due to a worldwide shortage of traditional energy sources, the DG sources incorporation has expanded dramatically in recent years. The usage of these resources is affected by a number of problems, such as their high upfront cost and the inability to manage environmental conditions like variations in wind and solar irradiation. Power should be shifted from one source to another using an intelligent energy control system that monitors the demand, the environment and the energy storage devices.

P. Pareek et al. (Eds.): IC4S 2023, LNICST 537, pp. 3–18, 2024.
https://doi.org/10.1007/978-3-031-48891-7_1

Altering the parameters of a hybrid renewable energy system (HRES), which draws power from many renewable resources, is best accomplished through the usage of a Microgrid. Controller settings, power management techniques, and system dimensions that maximize efficiency for HRES are the primary topic of a number of studies in the literature [1, 2]. In [2], hybrid Microgrid architecture was built out of photovoltaic (PV) and wind turbine (WT) generators. A mathematical steady-state model of the interconnected wind and solar Microgrid system was developed, and two different control mechanisms were implemented. This hybrid Microgrid model was simulated with the MATLAB/SIMULINK software. The best method for controlling the load was used. Many case studies including the relocation of sources and loads were carried out on the test system. The findings demonstrate that the system may be maintained in a steady-state condition by applying the proposed control methods while the network is changed from one operating condition to the next. In [3], the EMS is presented in the form of a Markov decision process (MDP). If you're dealing with an unpredictable situation, reinforcement learning is the way to go how effective data-driven method has also been enhanced by the creation of a comprehensive reward function that reduces the investigation of infeasible activities.

The findings demonstrate that the system may be maintained in a steady-state condition by applying the proposed control methods while the network is changed from one operating condition to the next. In [3], a Markov decision process model of the EMS is presented. Additional publications in the literature [4–6] typically concentrate on performance evaluation, converter design, and integrating renewable and conventional resources. Another alternative presented by the authors of [7] is the Smart Hybrid Energy System (SHES), which is a micro generation system meant to replace the existing diesel generator. To maximize the system's effectiveness, care must be taken with each component to guarantee a constant flow of power to the load. Mixed integer linear programming (MGEM) is used to operate a Microgrid, which is a type of hybrid energy system (HES) that combines sustainable sources like wind and solar with conventional power sources like photovoltaic cells, fuel cells, micro turbines, diesel, and energy storage. The HES's inability to effectively avoid pollution is exacerbated by its use of inefficient and environmentally damaging energy sources like diesel. Intelligent and smart controllers have an impact on HRES performance, although this impact is minimally defined or explained in the study. The topic of this research can be broken down further by the type of connected hybrid microgrid. Droop and power flow regulation are the primary areas of attention for the AC/DC microgrid's power management. For AC/DC grids can apply droop control [8–10]. If the latter is chosen, the interconnection between the two sub-grids is planned largely to deal with the case where a sub-grid fails due to overstress, while keeping adjustments to individual sources to a minimum [9]. By developing a sophisticated controller for a targeted hybrid DG, this study intends to close this gap. This work's key contribution may be summed up as follows: the study presented in this publication is the first to examine the feasibility of deploying a hybrid wind and photovoltaic system in off-grid settings.

This off-microgrid device uses a smart controller to programme in the desired characteristics [11]. When the amount of PV power is greater than the amount of power need to operate the load, the surplus required for alteration of batteries. Here energy produced by the PV is less, the stored energy is supports the requirements. The smart controller also prevents damage to the battery banks from rated, under/over-charging states. The controller must react appropriately in all cases. Whenever the SOC $< 81\%$, the wind turbine will automatically switch down before the PV panels. Before the SOC exceeds the controller-defined "safe margin," in this case 75%, the DG has disconnected. Additional commands to off loads and inverter are sent out the SOC $< 21\%$. After the battery is charged to 75% of its capacity, the inverter's power is cut. The hybrid energy system is mathematically described in portion 2 of the present work. The development of the proposed hybrid controller technique is discussed in portion 3. Portion 4 presents and discusses the results. Portion 5 lays out the major takeaways and directions for future research.

2 Suggested Microgrid System

The hybrid DG and the power electronic components that connect the both sides of AC/DC are the three main components of the system under investigation. Multiple controllers are required for high-powered electrical machinery. The Microgrid system configuration and diagram are depicted in Fig. 1. In the next portion, we'll go to the specifics of how each component is laid out. Figure 2 represents the analogous circuit of a PV cell.

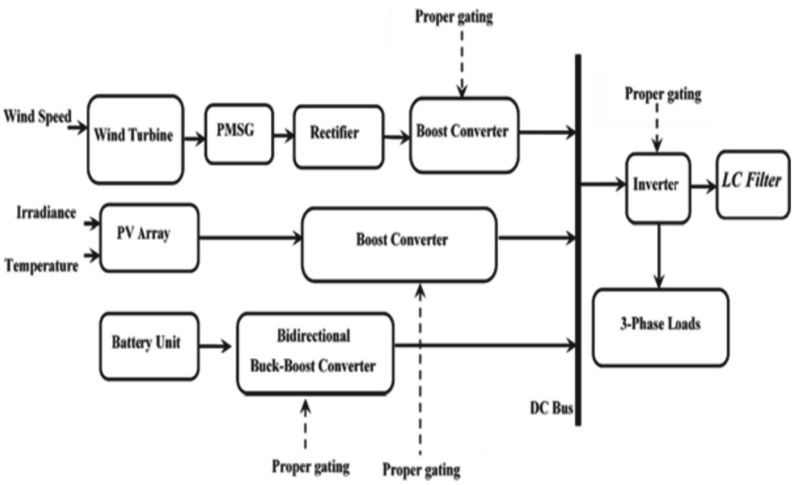

Fig. 1. Setup for the testing environment

From PV Curves

$$I_{pv} = I_{ph} - I_s e^{\left(\frac{q(V_{pv}+R_s I_{pv})}{nkT} - 1\right)} - \frac{V_{pv} + R_s I_{pv}}{R_{sh}} \quad (1)$$

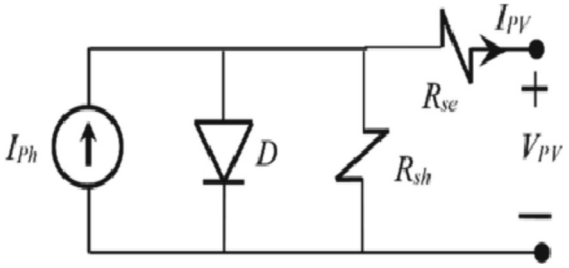

Fig. 2. Analogous circuit of a PV Cell

Where n represents the P-N junction's ideality factor, T represents the temperature in Kelvin. The combined PV system consists of a PV array with three 3 × 6 strings, capable of producing 3.91 kW at full irradiation of 1001 W/m^2. Figure 3 shows that the PV panel's open circuit voltage is very close to its maximum power output. This panel is rated at 215 W under standard test conditions. The open circuit voltage is 36.6, and the maximum power voltage is 29. Maximum point current is 7.35 A, while the short circuit current is 7.84 A. You can learn more about this panel and its features by consulting [12, 13].

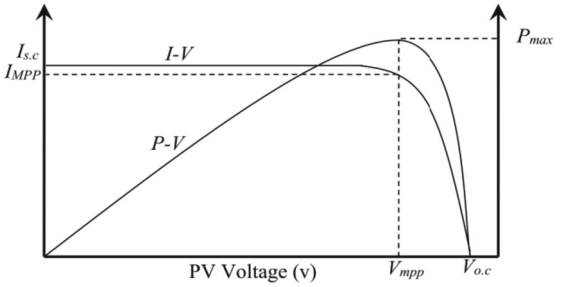

Fig. 3. Characteristics of a PV cell

2.1 WES with PMSG

All wind power systems require wind turbines. They act as the driving force for the electric generators that are mounted on their shafts. Wind turbines that rotate on different axes. The operating speed also categorizes devices into two groups: constant and variable. Figure 4 portrays the extracted mechanical power from the turbines. The P_{wind} is given by

$$P = 0.5 p_a A C_p v^3 \tag{2}$$

The aerodynamic power coefficient of a wind turbine is affected by the tip-speed ratio and the blade pitch angle, both of which are indicators of performance. Depending on the features of the turbine, a general equation for C_p is provided in (2) [14, 15].

$$C_\rho(\lambda, \boldsymbol{\beta}) = C_1\left(\frac{C_3}{\lambda_i} - C_3\beta - C_4\right)e^{\frac{-C_5}{\lambda_i}} + C_6\lambda \tag{3}$$

where C1 = 0.5176, C2 = 116, C3 = 0.4, C4 = 5, C5 = 21, and C6 = 0.0068, and

$$\lambda = \frac{\omega R}{V_w}$$
$$\frac{1}{\lambda_i} = \frac{1}{\lambda + 0.08\beta} - \frac{0.035}{\beta^3 + 1} \tag{4}$$

Turbine radius (R) is measured in meters; wind velocity (V_W) is measured in m/s; and angular velocity (ω) is measured in rad/s.

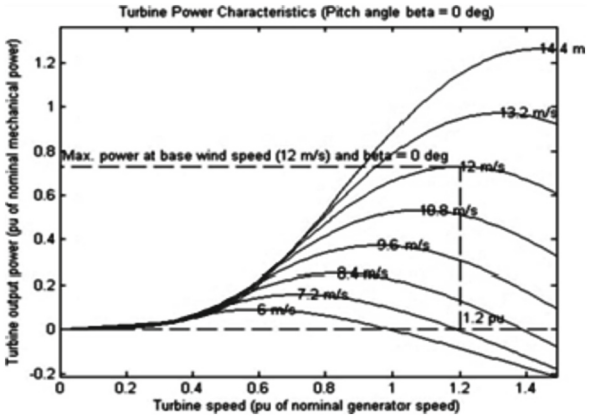

Fig. 4. Characteristics of wind turbine

2.2 Permanent Magnet Synchronous Generators

Various pole numbers are used in the construction of PMSG in WECS. To conserve energy, it operates at the same low speed as the wind turbine. Therefore, PMSG can be linked directly to the wind turbines rotor shaft. Direct-drive operation is an example of this sort of operation because it does not require the installation of a gearbox [16]. The system offers a benefit over DFIG-based systems, which call for a gearbox, in terms of both installation and maintenance costs due to the elimination of gears. The PMSG is flexible in its ability to accommodate varying rotor speeds. The frequency and amplitude of the voltage delivered to the PMSG's stator terminals vary with the Vw. The power converters being used are rated at full capacity, allowing for the most efficient conversion of wind energy possible throughout a broad range of wind speeds in the absence of any extra rotor control. Full-rated power converters not only help in conforming to a variety of grid requirements, but also eliminate the need for extra hardware in fault ride-through situations [17–19]. Figure 5 shows the basic wind energy systems.

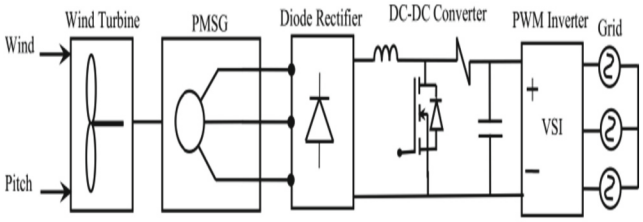

Fig. 5. Standard wind energy conversion using PMSGs

2.3 Battery-Powered Bidirectional DC-DC Converter

The usage of lead-acid batteries is widespread in PV power systems. A bidirectional DC-DC converter is used to charge and discharge these batteries. The authors of [15, 16] explore bidirectional DC-DC converter architectures and combinations for use in PV systems. The buck and boost processes in this investigation make use of a bidirectional chopper. The bidirectional converter in its most frequent design, as reported in this study, is depicted in Fig. 6. Switch S1 receives the gate signal, turning the bidirectional converter into a buck converter. When the PV output is high, the battery system will enter this mode to charge the batteries. When energy is low from the PV system or the grid, the bidirectional converter can function as a boost converter by delivering a gate signal to switch S2. This causes the battery to deplete and the load to be supplied with power. Parameters for a bidirectional converter are developed using expressions.

$$C_H = \frac{D}{R_H f_s \left(\Delta \frac{V_H}{V_H}\right)}$$
$$L_{b,min} \geq \frac{D(1-D)^2 R_H}{2f_s} \tag{5}$$

Here RL& RH are the load resistances of bidirectional chopper, respectively. Boost side capacitance is denoted by CH. The minimum value of the inductance is Lb, min, and the switching frequency is FS. Microgrids have various features, which are detailed in Table 1.

Buck Mode:

$$L_{b,min} \geq \frac{(1-D)R_L}{2f_s} \tag{6}$$

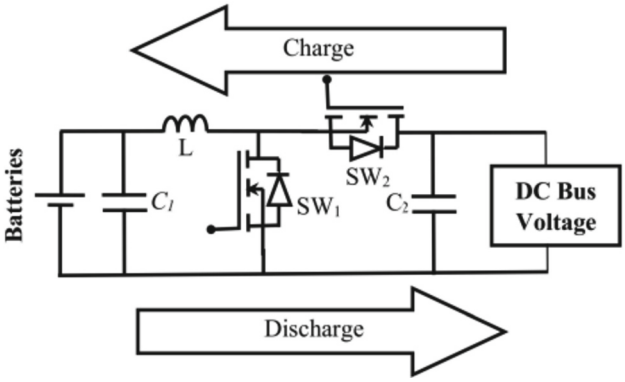

Fig. 6. Bidirectional buck–boost converter

Table 1. Sizing and specifications of the microgrid system.

Load Sizing	DC Bus Voltage	700 Vdc
	Load Power Required	2 kW
Battery Sizing	Batteries capacity	102 Ah
	Battery Voltage	96 Vdc
	Batteries capacity	9.8 kWh
	Batteries strings (parallel)	1
	Batteries per string (series)	4
PV Array Sizing	PV Module	Soltech 1STH-215-P
	Max Power Per Module	213 W
	Max Current	7.35 A
	Max Voltage	29 V
	Parallel Strings	6
	Series Modules per string	3
PMSG	Rated Power	3 kW
	Rated Speed	360 RPM

Table 2. Comparision for praposed and conventional system Performance

	ANFIS based IFO-PID	IFO-PID
Wind Power (W)	9950	9800
PV Power (W)	3300	3000
SSCs Power (W)	13500	13000
Battery Stored Power (W)	2600	2500
Battery Supplied Power (W)	4700	4500

3 ANFIS Model

The rules can be created using a decomposition method thanks to the ANFIS structure. ANFIS is a feed-forward network with multiple layer with adaptive and fixed nodes, each of which has a defined role to carry out on the incoming signals. In order to capture the system's overall dynamics, the rules are first extracted from the neural network at the level of each individual node. The predetermined input-output pairings are produced by fuzzy if-then rules with suitable affiliation functions, and these membership functions take on their final forms during training as a result of regression and optimization techniques.

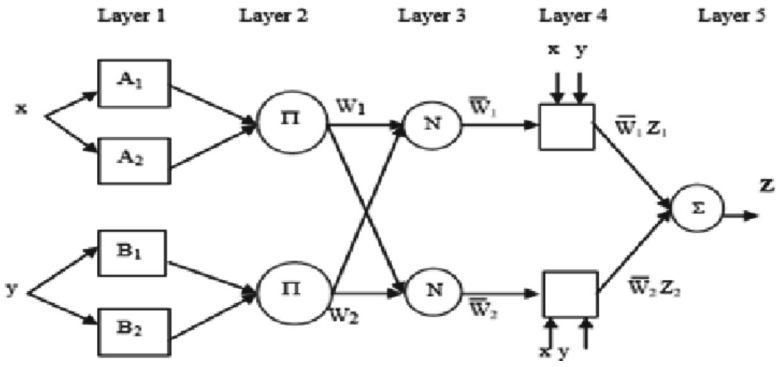

Fig. 7. ANFIS model

A gauge of how effectively the system is simulating the given training data set for a particular set of parameters is provided by the gradient vector (Fig. 7). After obtaining the gradient vector, optimization techniques are used to modify the parameters in order to lower a specified error criterion. When the training and checking errors are under a certain threshold, the system converges. Since the blind control system in this situation is thought of as a first order system, a first order Sugeno fuzzy model will be used to describe it. Due to its transparency and effectiveness, we will use the first order Sugeno fuzzy model for the dynamic application. Sugeno models of higher order complicate the system without adding much value. So, a first order system is used to create the blind control system.

4 Simulation Outcomes

Microgrid system was developed and two different control mechanisms were implemented. This hybrid Microgrid model was simulated with the MATLAB/SIMULINK software and the respective results are shown in Figs. 8, 9, 10, 11, 12, 13, 14, 15, 16, 17, 18, 19, 20. The suggested system's simulation results can be found in below references, along with the parameters that were employed. DC-link fixed-value reference to 240 V. The results of the energy management unit focus of the simulation test. Firstly, at an initial state of charge (SOC) of 80%, the BSS connects of DC load of 8000 watts to the DC-link through two load-side converters. The wind prole among 8 as well as 13 m/s is seen in Fig. 8. Figure 14 depicts the range of wind power (in watts) produced, that is 4000 to 10000 (based on wind speed). At 25°C and a brightness of 600 W per square meter, a PV array can provide 3000 W of power, as depicted in Fig. 10. The combined photovoltaic and wind power generation Pdg is shown in Fig. 11. Current responses place the range of Pdg produced power at among 7,000 as well as 13,000.

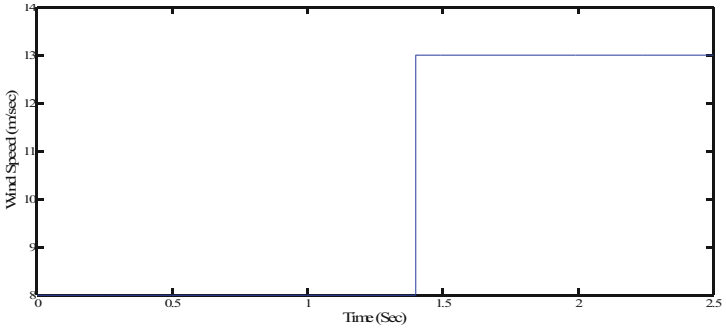

Fig. 8. Wind Speed

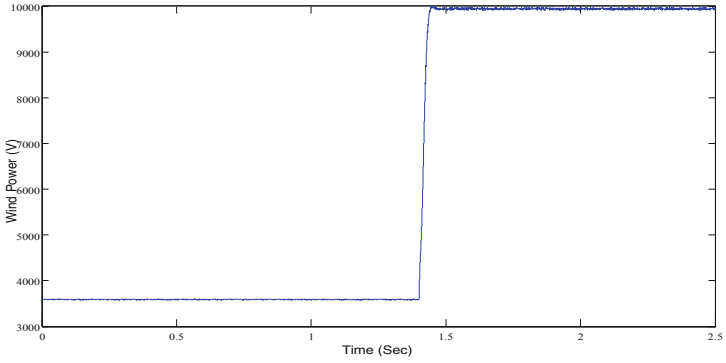

Fig. 9. Wind Power

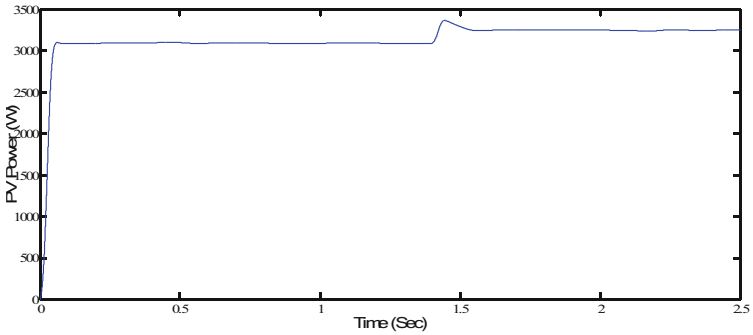

Fig. 10. PV Power

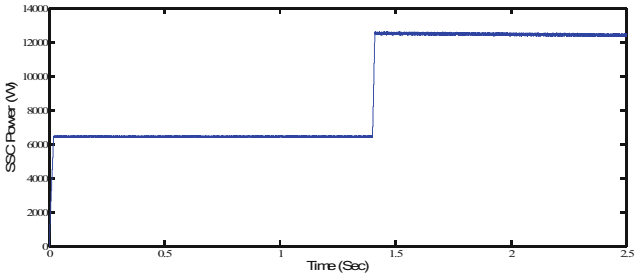

Fig. 11. SSC's Power

Battery capacity and state of charge are displayed in Figs. 12 and 13. When SOC is greater than 20%, the findings show that the battery feeds the microgrid with around 2300 W during the [0–1.4] s period, while the generated Pdg is greater than the load power during the [1.4–2.3] s interval. That's why the microgrid supplies around 4500 W to the battery during a charge. It is clear from comparing the DC-link voltage of the SSCs and LSCs in Fig. 14 that both the PI and the proposed ANFIS based IFO-PID maintain the DC-link at its reference value. While other PID controllers struggle with steady-state errors and convergence, the suggested IFO-PID consistently outperforms the competition.

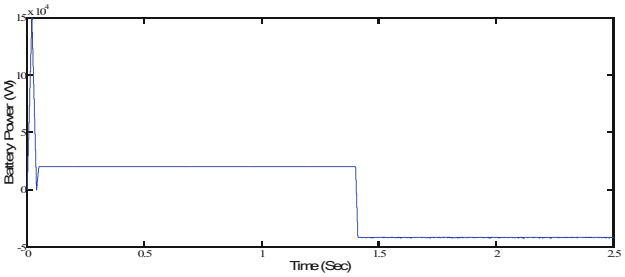

Fig. 12. Battery Power

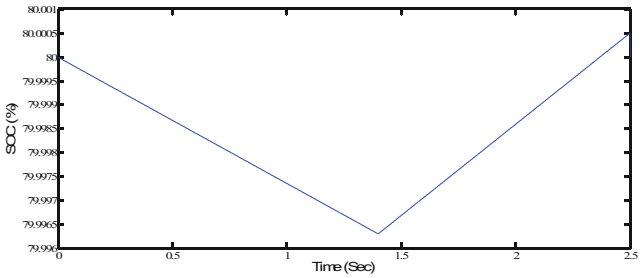

Fig. 13. SOC

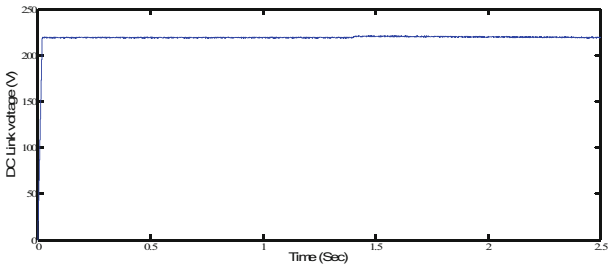

Fig. 14. DC Link Voltage

BSS power, seen in Fig. 12 If you look at Fig. 15, you can see that the proposed energy management system always sends the same 8300 W to the loads. As can be seen in Fig. 16, the suggested ANFIS based IFO-PID is able to maintain a constant output voltage of 220 V. In this subsection, the benefits of the proposed ANFIS based IFO-PID are highlighted by comparing them to those of prior works. Table 2 displays the results of this comparison, ANFIS based IFO-PID and IFO-PID revealing that the suggested method generates more power and shows good performance when compared to the compared control schemes. The proposed control technique effectively handled the hybrid energy, and the goals were met. Current work's load voltage compares favorably to prior approaches and demonstrates improved performance.

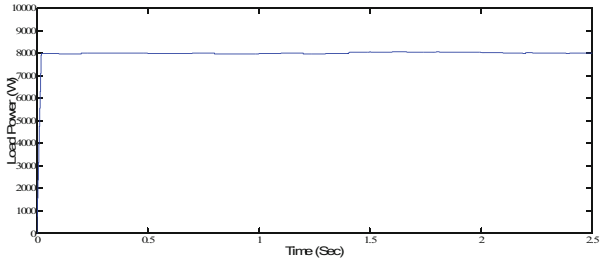

Fig. 15. Load Power

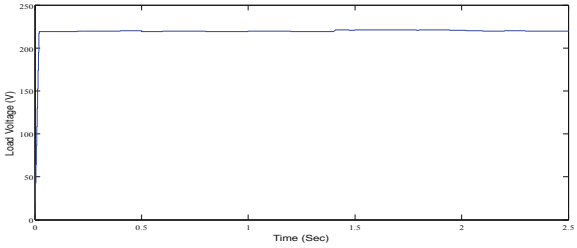

Fig. 16. Load Voltage

The proposed energy management technique is put to the test in Figs. 17 and 18 by simulating a random fluctuation in wind speed and solar radiation. The wind power output during variable wind conditions is depicted in Fig. 19. From what has been stated, it seems that the wind system can be used for MPPT. Figure 20 shows how the maximum power point tracking (MPPT) control ensures that the PV panel always extracts the greatest possible power from the sun.

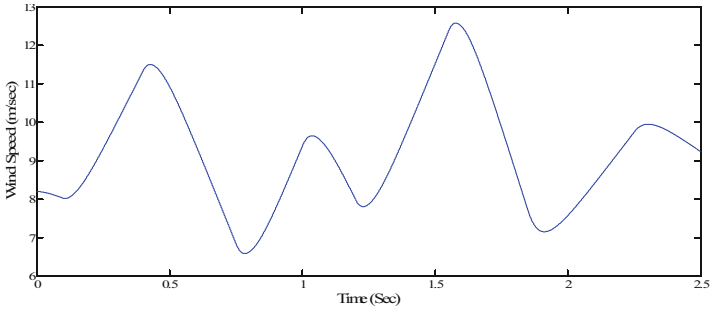

Fig. 17. Wind Speed

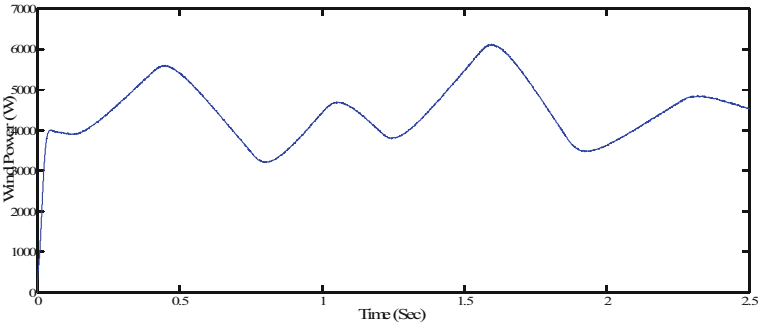

Fig. 18. Wind Power

The combined output of PV and wind is displayed in Fig. 20. As can be observed in Fig. 11, the results show that the output power remains constant at among 5000 as well as

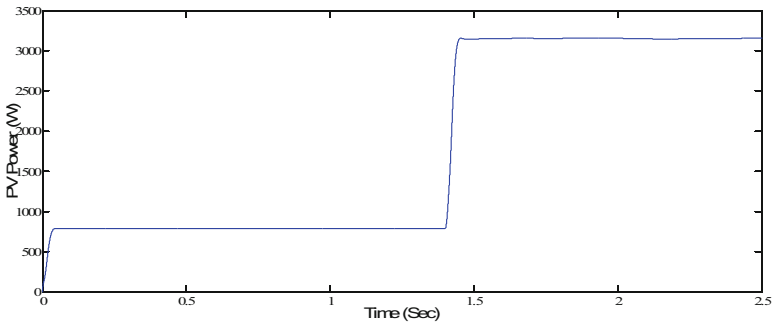

Fig. 19. PV Power

13000 W. The BSS is completely functional in energizing and using mode, and Fig. 21 depicts the power output when subject to random fluctuations. The recommended energy management control to transfer a uniform power to the load of around 8300 W. At last, we have the DC-link voltage response and the load power is plotted out in Fig. 22–23. The reported response demonstrates that the suggested method successfully controls the DC voltage at the specified reference. Consequently, the suggested energy management method assures continuous service and a steady supply of electricity, despite the inevitable fluctuations that are inevitable in any system.

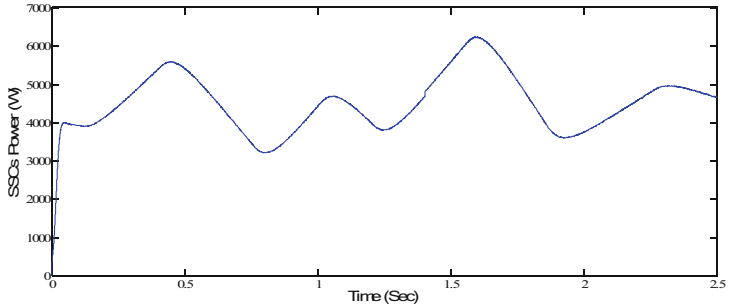

Fig. 20. SSC's Power

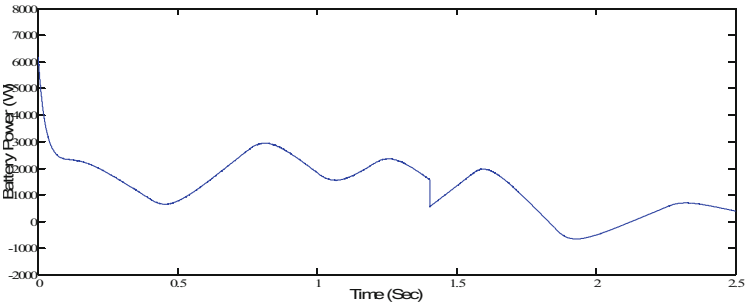

Fig. 21. Battery Power

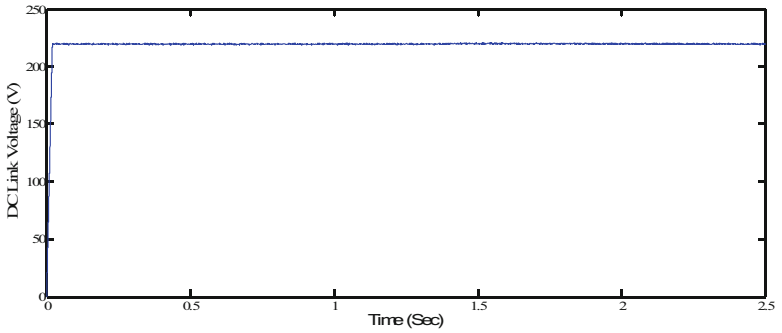

Fig. 22. DC Link Voltage

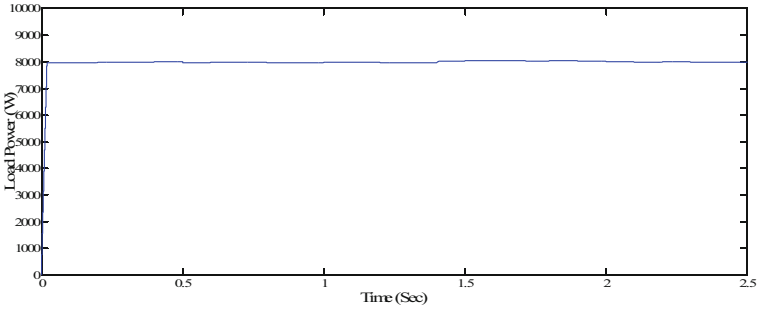

Fig. 23. Load Power

5 Conclusion

A PV system and WECS are suggested for use in the design and control of an independent micro-grid in this paper. The boost converter's control and optimization of power harvesting of PPV was achieved using MPPT with FLC. Here 2 controllers are employed to maintain a stable voltage from the PV to the battery storage system. The goal of controllers is continuously connect to the load. When the solar panels produce more power

than is needed, any excess is stored in batteries. The controllers are manages the battery and PV power under dynamic conditions. The controller's actions must be appropriate in every scenario. The controller will not depend on SOC and operates as normal while typical working conditions (21% SOC 81%). When the SOC drops to 81%, a precise instruction is issued to turn off the wind turbine and solar panels. Connecting the wind mill energy and PV modules energy is not possible until the SOC in this controller falls below 75%. When the SOC > 21%, other hand it controls load and inverter. Once the batteries are fully charged, power is restored to the inverter. The problem was resolved by the built independent Microgrid system and associated controllers, which brought electricity to previously unconnected locations. Input penetrations in grid-connected mode of operation, as well as the functionality of the proposed system during fault conditions, will be the focus of future research.

References

1. Pareek, P., Maurya, N.K., Singh, L., Gupta, N., Reis, M.J.C.S.: Study of smart city compatible monolithic quantum well photodetector. In: International Conference on Cognitive Computing and Cyber Physical Systems, pp. 215–224 (2022)
2. Mangu, B., Akshatha, S., Suryanarayana, D., Fernandes, B.G.: Grid-connected PV-wind-battery-based multi-input transformer-coupled bidirectional DC-DC converter for household applications. IEEE J. Emerg. Select. Top. Power Electron. **4**(3), 1086–1095 (2016)
3. Roselyn, J.P., et al.: Design and implementation of fuzzy logic based modified real-reactive power control of inverter for low voltage ride through enhancement in grid connected solar PV system. Control. Eng. Pract. **101**, 104494 (2020)
4. Divyasharon, R., Banu, R.N., Devaraj, D.: Artificial neural network based MPPT with CUK converter topology for PV systems under varying climatic conditions. In: 2019 IEEE International Conference on Intelligent Techniques in Control, Optimization and Signal Processing (INCOS), pp. 1–6 (2019)
5. Zou, H., Du, H., Ren, J., Sovacool, B.K., Zhang, Y., Mao, G.: Market dynamics, innovation, and transition in China's solar photovoltaic (PV) industry: a critical review. Renew. Sustain. Energy Rev. **69**, 197–206 (2017)
6. Wang, P., Wang, W., Meng, N., Xu, D.: Multi-objective energy management system for DC microgrids based on the maximum membership degree principle. J. Modern Power Syst. Clean Energy **6**(4), 668–678 (2018)
7. Garmabdari, R., Moghimi, M., Yang, F., Gray, E., Lu, J.: Multi-objective energy storage capacity optimisation considering microgrid generation uncertainties. Int. J. Electr. Power Energy Syst. **119**, 105908 (2020)
8. NajiAlhasnawi, B., Jasim, B.H., Esteban, M.D.: A new robust energy management and control strategy for a hybrid microgrid system based on green energy. Sustainability **12**(14), 57249 (2020)
9. Zhang, Y., Liu, B., Zhang, T., Guo, B.: An intelligent control strategy of battery energy storage system for microgrid energy management under forecast uncertainties. Int. J. Electrochem. Sci. **9**(8), 4190–4204 (2014)
10. Shadmand, M.B., Balog, R.S.: Multi-objective optimization and design of photovoltaic-wind hybrid system for community smart DC microgrid. IEEE Trans. Smart Grid **5**(5), 2635–2643 (2014)
11. Pragaspathy, S., Karthikeyan, V., Kannan, R., Korlepara, N.D.P., Krishna, B.: Photovoltaic-based hybrid integration of DC microgrid into public ported electric vehicle. In: Wind and Solar Energy Applications, CRC Press, Tailor and Francis, pp. 287–303 (2023)

12. Bheemraj, T.S., Kumar, Y.A., Karthikeyan, V., Pragaspathy, S.: A hybrid structured high step-up DC-DC converter for integration of energy storage systems in military applications. IEEE Trans. Circuits Syst. II Express Briefs **70**(4), 1545–1549 (2022)
13. Nalli, P.K., Kadali, K.S., Bhukya, R., Palleswari, Y.T.R., Siva, A., Pragaspathy, S.: Design of exponentially weighted median filter cascaded with adaptive median filter. J. Phys. Conf. Ser. **2089**(1), 012020 (2021)
14. Chakravarthi, B.N.C.V., Hari Prasad, L., Chavakula, R.L., VijethaInti, V.V.: Solar energy conversion techniques and practical approaches to design solar PV power station. In: Sustainable and Clean Energy Production Technologies, Springer Nature Singapore, pp. 179–201 (2022)
15. Kannan, R., Karthikkumar, S., Suseendhar, P., Pragaspathy, S., Chakravarthi, B.C.V., Swamy, B.: Hybrid renewable energy fed battery electric vehicle charging station. In: 2021 Second International Conference on Electronics and Sustainable Communication Systems (ICESC), pp. 151–156 (2021)
16. Samy, M.M., Mosaad, M.I., Barakat, S.: Optimal economic study of hybrid PV-wind-fuel cell system integrated to unreliable electric utility using hybrid search optimization technique. Int. J. Hydrogen Energy **46**(20), 11217–11231 (2021)
17. Babatunde, O.M., Munda, J.L., Hamam, Y.: Hybridized off-grid fuel cell/wind/solar PV/battery for energy generation in a small household: a multi-criteria perspective. Int. J. Hydrogen Energy **47**(10), 6437–6452 (2022)
18. Kasireddy, I., Nasir, A.W., Singh, A.K.: Application of FOPID-FOF controller based on IMC theory for automatic generation control of power system. IETE J. Res. **68**(3), 2204–2219 (2019)
19. Gupta, N.K., Kasireddy, I., Singh, A.K.: Design of PID controller using strawberry algorithm for load frequency control of multi-area interconnected power system with and without non-linearity. In: Control Applications in Modern Power Systems: Select Proceedings of EPREC, vol. 870, pp. 153–162 (2022)